Research Article

Shanxiu Huang, Huikuan Li, Fenghui Gao*, Weijie Guo, and Jiaqi Guo

Optimization of preparation parameters and testing verification of carbon nanotube suspensions used in concrete

https://doi.org/10.1515/ntrev-2024-0124 received June 28, 2024; accepted October 24, 2024

Abstract: Carbon nanotubes (CNTs) have received extensive attention due to their exceptional properties and wide range of applications. However, the agglomeration of CNTs in aqueous solutions and organic solvents significantly limits their large-scale application. In this study, the microscopic morphology and dispersion stability of the CNT suspensions were analyzed, and the most suitable surfactant in this study was selected. The preparation parameters of the CNT suspensions were optimized, and uniaxial compression tests were conducted on carbon nanotube concrete (CNTC) prepared using the optimized parameters. Scanning electron microscope analysis was used to investigate the improvement in the microstructure of the concrete by CNTs. Transmission electron microscope micrographs of the polyvinyl pyrrolidone (PVP)-CNT suspensions exhibited a uniformly distributed CNT cross-linked network. The absorbance reduction ratio of PVP-CNT suspensions after standing for 90 days was 13.75 and 22.41%, respectively. The absorbance reduction ratio of the suspensions first increased and then decreased with increasing dispersant ratio and ultrasonic dispersion time and increased with increasing ultrasonic power ratio. Compared with that of plain concrete, the uniaxial compressive strength of CNTC significantly improved, with a maximum increase of 18.15% when the content was 0.10%, and the failure mode exhibited typical shear failure characteristics. The optimized preparation

Jiaqi Guo: School of Civil Engineering, Henan Polytechnic University, Jiaozuo, 454003, China

China

parameters for the CNT suspensions were a PVP-to-multiwalled carbon nanotube mass ratio of 4:1, an ultrasonic dispersion time of 20 min, and an ultrasonic power of 60%. These optimized parameters are ideal choices for preparing CNT cement-based composite suspensions.

Keywords: carbon nanotube, suspension, dispersion stability, compressive strength

1 Introduction

As the most widely used traditional building material in the world, concrete boasts various advantages, such as low cost, abundant resources, and good compression resistance. It plays a pivotal role in engineering construction and is expected to continue to play an indispensable key role in the future. However, with the rapid economic development and improvements in scientific and technological strength, the architectural structures involved in modern mining engineering, bridge engineering, urban construction engineering, railway engineering, and basic engineering fields of the machinery manufacturing industry in China have begun to develop rapidly in the direction of large-span, super-high, super-deep, and multifunctionalization techniques. The performance and function of traditional building materials can no longer meet people's requirements for new architectural structures. At the same time, the harsh and complex service environments lead to a decrease in the mechanical properties, resistance attenuation, and service life of architectural structures [1,2]. Therefore, research on high-performance cement-based materials with the development of sustainability, intelligence, super durability, and multifunctionalization has become a popular topic in materials science and engineering. Chung [3] and Li et al. [4] first carried out research on self-sensing carbon fiber cement-based composite materials. Zhou and Yang studied the sensing properties of nylon fiber cement-based composite materials with carbon coatings in 2001 [5]. Li et al. proposed the application of steel slag cement-based

^{*} Corresponding author: Fenghui Gao, Henan First Geology and Mineral Survey Institute Co., Ltd., Luoyang, 471023, China; Key Laboratory of Au-Ag-Polymetallic Deposit Series and Deep-seated Metallogenic Prognosis of Henan Province, Luoyang, 471023, China; Key Laboratory of Precious Metals Analysis and Exploration Technology, MNR, Luoyang, 471023, China, e-mail: wyqwyx001@163.com Shanxiu Huang, Huikuan Li, Weijie Guo: School of Chemistry and Chemical Engineering, Henan Polytechnic University, Jiaozuo, 454003,

2 — Shanxiu Huang et al. DE GRUYTER

composite materials in 2005 [6]. Kim *et al.* prepared engineered cement-based composite materials produced by grinding blast furnace slag in 2007 and conducted single-fiber pull-out tests and matrix fracture tests [7]. In 2008, Sivakumar *et al.* studied the hydration rate of fly ash mixed cement composite materials in the early stage using fly ash as a filler [8]. Xiong *et al.* studied the microwave absorption and mechanical properties of nanotitanium oxide cement-based composite materials in 2010 [9]. Wang *et al.* prepared basalt fiber concrete beams with volume ratios of 0.1 and 0.2% in 2011 and conducted bending tests [10].

As seen from the above research, new fillers are constantly being used to prepare high-performance cementbased composite materials [11,12]. In 1991, the Japanese scientist Iijima discovered that carbon nanotubes (CNTs) have excellent mechanical properties, high chemical and thermal stability, low resistivity, and electromagnetic wave absorption properties due to their special internal structure, making them ideal reinforcing materials for various matrix materials [13-16]. The combination of CNTs and concrete can effectively utilize the excellent mechanical and electrical properties of CNTs, significantly improve the low toughness and high brittleness of concrete, and endow concrete with good mechanical and electrical properties and unique self-sensing effects [17–21]. In the process of preparing carbon nanotube concrete (CNTC), the addition of a small amount (not more than 0.5% of the cement mass) of CNT can achieve a strong composite effect. However, due to the large aspect ratio of CNTs and the strong van der Waals forces between the tube walls, CNTs are prone to agglomerate and form large clusters, resulting in CNTs not being uniformly dispersed in cement-based composite materials. This leads to the actual reinforcement effect of CNT concrete not reaching the theoretical expectation. Therefore, preparing an aqueous suspension that can uniformly and stably disperse CNTs into cement-based materials is an important prerequisite for obtaining highquality CNTC. Cwirzen et al. used polyacrylic acid polymer as a dispersant and achieved good results after ultrasonic treatment and dispersion of CNTs [22]. Xin et al. used organosilicon surfactants as CNT dispersants, and the research showed that the hydrophilic polyethylene part of the surfactant enables the dispersion of CNTs in aqueous solutions through spatial stabilization [23]. Li et al. [24] and Yazdanbakhsh et al. [25] found that ultrasonic waves and surfactant technology can achieve uniform dispersion of CNTs in cement-based materials. However, excessive ultrasonic energy can lead to CNT breakage, and improper use of surfactants can delay or even stop the cement hydration and hardening process. Makar et al. [26] and An et al. [27] showed that using surfactants and ultrasonic dispersion technology can achieve good dispersion of CNTs

in aqueous systems, and the ratio of dispersants to CNTs significantly affects the dispersibility of CNTs in cement-based materials. Bu *et al.* used sodium dodecyl benzene sulfonate (SDBS) as a dispersant and a choline chloride-malonic acid ionic liquid as a solvent to prepare a well-dispersed CNT suspension through ultrasonic dispersion of CNTs [28].

In summary, the combination of surfactants and ultrasonic dispersion is a common and feasible technology. However, in this technology, the selection of suitable dispersants and the optimization of various process parameters during the preparation of CNT suspensions have vet to be determined. Currently, few systematic studies analyze the dispersion effect and stability of suspensions from multiple perspectives. Therefore, this study investigated the microscopic morphology and stability of CNT suspensions under natural standing and centrifugal separation conditions, optimized the parameters for preparing CNT suspensions using a combination of ultrasonication and surfactants, and performed uniaxial compression tests on CNTC. Scanning electron microscope (SEM) analysis was utilized to reveal the microscopic mechanism by which CNTs improve the mechanical properties of concrete. The research findings enrich and improve the theoretical system research on the dispersion stability of CNT suspensions, providing an important reference and significance for the engineering application of CNT cement-based materials.

2 Experimental program

2.1 Materials

Multiwalled carbon nanotubes (MWCNTs), prepared by chemical vapor deposition at the Chengdu Institute of Organic Chemistry, Chinese Academy of Sciences, are black powders with purities greater than 90%, specific surface areas ranging from 230 to 280 m²/g, electrical conductivities greater than 100 S/m, a diameter of 10-20 nm, and a length of less than 30 µm, as shown in Figure 1(a). Polyvinyl pyrrolidone (PVP), which was produced by Sinopharm Chemical Reagent Co., Ltd., in Shanghai, is a nonionic surfactant in the form of a white or slightly yellow powder, with an ignition residue of no more than 0.1%, a total nitrogen content of 11.5–12.8%, a K value of 27.0–32.4%, and a moisture content of no more than 5.0%, as depicted in Figure 1(b). SDBS, also produced by Sinopharm Chemical Reagent Co., Ltd., in Shanghai, is an anionic surfactant in the form of a white powder that is soluble in water; it contains moisture and volatiles of no more than 5.0% and sodium sulfate of no more than 9.0%, as shown in Figure 1(c). Gum arabic (GA) was produced by Xilong Science



Figure 1: MWCNTs and dispersants. (a) MWCNTs, (b) PVP, (c) SDBS, and (d) GA.

Co., Ltd., and is a nonionic surfactant that is a yellowish powder and is soluble in water; it has a relative density ranging from 1.35 to 1.49, a loss on drying of no more than 10.0%, and an ignition residue of no more than 4.0%, as shown in Figure 1(d).

The coarse aggregates selected were continuously graded crushed stone with a specific gravity of 2.56 and a particle size ranging from 5 to 20 mm, complying with the standard GB/T 14685-2011 [29]. The fine aggregates are natural medium-coarse river sand with a fineness modulus of 2.6 and a particle size ranging from 0.15 to 4.75 mm, complying with the standard GB/T 14684-2011 [30]. The cement used is ordinary Portland cement produced by Jiaozuo Qianye Cement Co., Ltd., complying with the standard GB 175-2007 [31]. The mixing water is drinking water produced by Jiaozuo Water Supply Co., Ltd., which contains few impurities and does not adversely affect the performance of CNTC.

2.2 Preparation and characterization of CNT suspensions

First, surfactants were added to a beaker filled with distilled water and stirred with a glass rod until completely dissolved. Then, a certain amount of CNTs was added to each surfactant solution. After initial stirring using an HJ-

4B magnetic stirrer, the mixture was transferred to a Y92-II ultrasonic cell crusher for ultrasonic dispersion. After dispersion, the beaker was covered with plastic film for future use, as shown in Figure 2(a). A UV-3600 ultraviolet spectrophotometer was used to measure the absorbance of the CNT suspensions prepared with different surfactants. The absorbance was used to characterize the dispersion effect and stability of the CNT suspensions under different conditions. According to the Beer-Lambert law,

$$A = \log \frac{1}{T} = Ecl. (1)$$

The absorbance A of the solution is proportional to the product of the concentration c and path l of the solution. For a certain optical path, the concentration of the CNT suspension was calculated according to the absorbance of the measured CNT suspension to quantitatively characterize the relationship between the CNT content and different dispersants to determine the dispersion effect of the CNT suspension [32,33]. The specific process for measuring the absorbance of the CNT suspension was as follows: (1) A CNT suspension with a concentration ranging from 0 to 0.1 g/L was prepared, and an aqueous dispersant solution with the same concentration as the reference solution was prepared. (2) The upper layer of 4 — Shanxiu Huang et al. DE GRUYTER

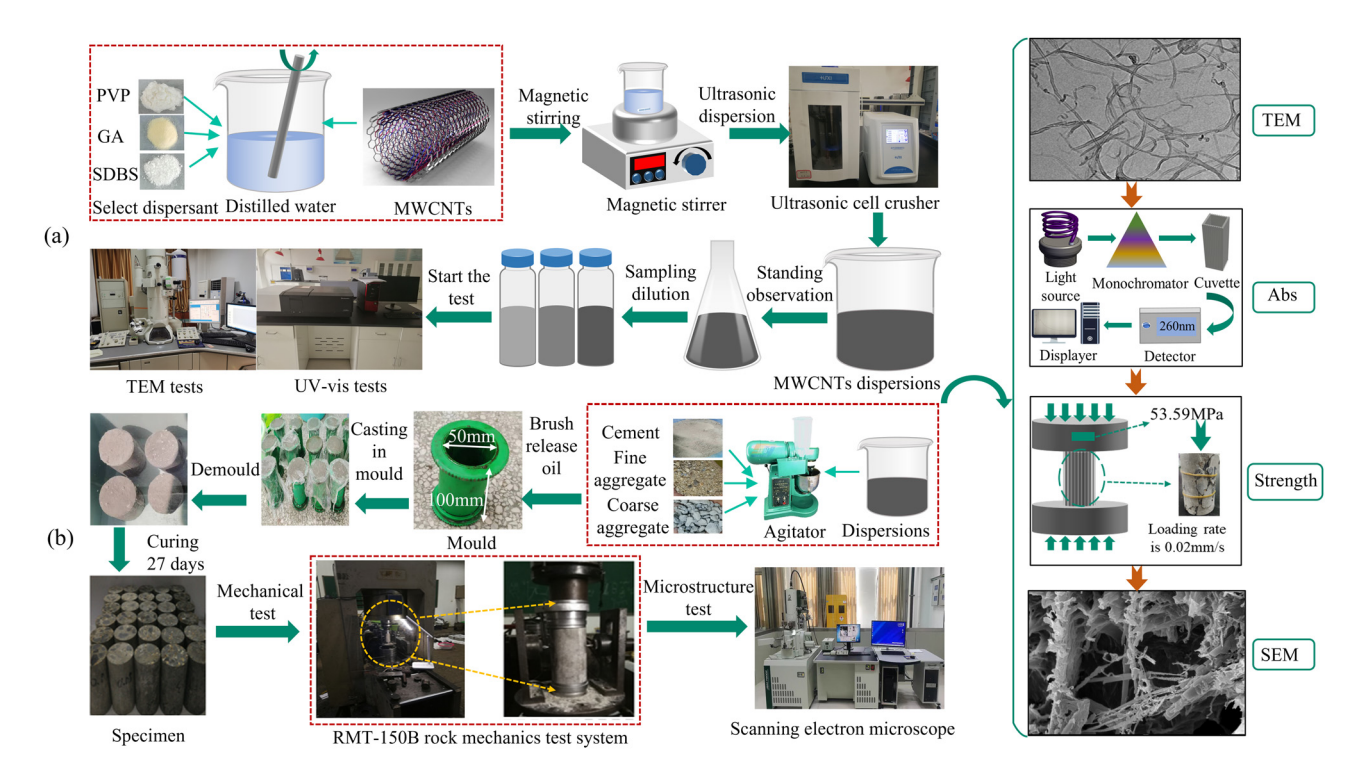


Figure 2: Test procedure: (a) suspension preparation and test and (b) sample preparation and test.

the CNT suspension containing different surfactants was removed, and the same concentration of surfactant aqueous solution was used as a reference. The absorbance at a wavelength of 260 nm was measured. A small amount of the prepared CNT-suspended droplets were absorbed on a copper grid with a carbon film, and the microscopic morphology of the CNT dispersion was observed by a Tecnai G2 F20 transmission electron microscope (TEM) after drying.

2.3 Experimental scheme for optimizing the preparation parameters of the CNT suspension

In this article, a CNT suspension was prepared using a combination of ultrasonic waves and surfactants. Three surfactants, SDBS, GA, and PVP, were selected for the surfactant optimization experiments. Based on the morphologies observed by TEM and suspension stability comparisons, the surfactant suitable for the CNTs used in this study was optimized. The experimental scheme is shown in Table 1, with a total of six groups of CNT suspensions. After determining a suitable surfactant for the CNT suspension, a reasonable ratio and process parameters for the ultrasonic dispersion of CNTs were determined through orthogonal experiments and intuitive analysis of the experimental results. The focus was on investigating the effects of a reasonable mass ratio of dispersant to CNTs,

ultrasonic dispersion time, and ultrasonic power on the stability of the CNT suspension. Three levels were used for each factor, and the interaction of influencing factors was not considered. The entire experimental process was conducted according to an orthogonal table ($L9(3^4)$). The orthogonal experiment factor levels are shown in Table 2.

3 Results and discussion

3.1 Influence of different dispersants on the morphology of CNT suspensions observed by TEM

When the CNT content was 0.02 g, the ultrasonic dispersion time was 30 min, and the ultrasonic power ratio was 40%,

Table 1: Experimental scheme used to optimize the surfactants

| Number | MWCNTs (g) | Surfactant (g) | Water (mL) | |
|--------|------------|----------------|------------|--|
| 1 | 0.02 | PVP 0.1 | 20 | |
| 2 | 0.05 | PVP 0.1 | 20 | |
| 3 | 0.02 | SDBS 0.1 | 20 | |
| 4 | 0.05 | SDBS 0.1 | 20 | |
| 5 | 0.02 | GA 0.1 | 20 | |
| 6 | 0.05 | GA 0.1 | 20 | |
| | | | | |

Table 2: Testing factor for preparation of the CNT suspensions

| Mass ratio of dispersant to CNT (A) | Ultrasonic time/ min (B) | Ultrasonic power ratio/% (C) |
|--|-----------------------------|------------------------------|
| 2:1 (A ₁) | 10 (B ₁) | 20 (C ₁) |
| 4:1 (A ₂) | 20 (B ₂) | 40 (C ₂) |
| 6:1 (A ₃) | 30 (B ₃) | 60 (C ₃) |

the dispersants had a significant impact on the micromorphology of the CNT suspension observed by TEM, as shown in Figure 3. According to the micromorphology of the CNT suspension with PVP as the dispersant, a uniformly distributed CNT cross-linked network is clearly visible, as shown in Figure 3(a). In the TEM images of the micromorphology of the CNT suspensions with GA and SDBS as dispersants, the CNTs agglomerated and entangled to form bundles, as shown in Figure 3(b) and (c), respectively. The agglomeration and entanglement phenomena in the CNT suspension with SDBS as the dispersant are more serious. Therefore, the dispersion effect of PVP, GA, and SDBS decreases successively.

When the CNT content increases to 0.05 g, the micromorphology of the CNT suspension with different dispersants is shown in Figure 4. According to the TEM images of the CNT suspension with PVP as the dispersant, the number and density of CNTs are significantly greater than those shown in Figure 3(a), showing a uniformly distributed cross-linked network of CNTs. The good dispersion effect of PVP benefits from the mutual attraction between the hydrophobic groups of nonionic surfactant molecules and the hydrophobic surface of CNTs, in which the surface of the CNTs encased in a layer of PVP molecular film. The steric hindrance effect overcomes the van der Waals forces between CNTs, preventing their agglomeration. Moreover, the hydrophilic groups of PVP endow PVP with a stronger dispersion ability. This is consistent with the research results of Kim et al. [34]. However, when GA, which is also a nonionic surfactant, is used as a dispersant, the TEM image shows local agglomeration of the CNT network, indicating that the van der Waals forces between CNTs are not yet effectively balanced, leading to a significant decrease in the uniform distribution of CNTs and resulting in the irregular network structure of the CNTs [35], as

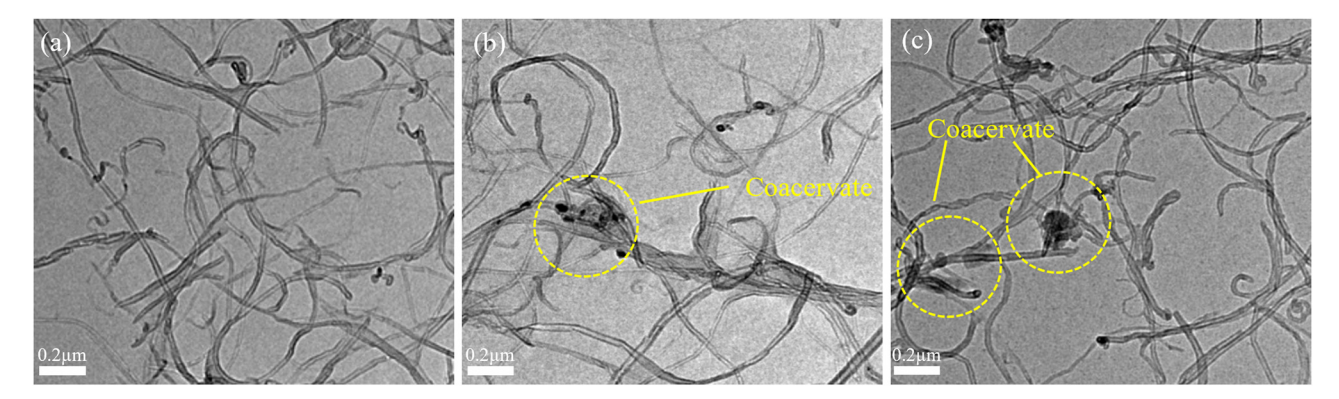


Figure 3: TEM images of CNT suspensions (0.02 g of CNTs) with different dispersants: (a) PVP, (b) GA, and (c) SDBS.

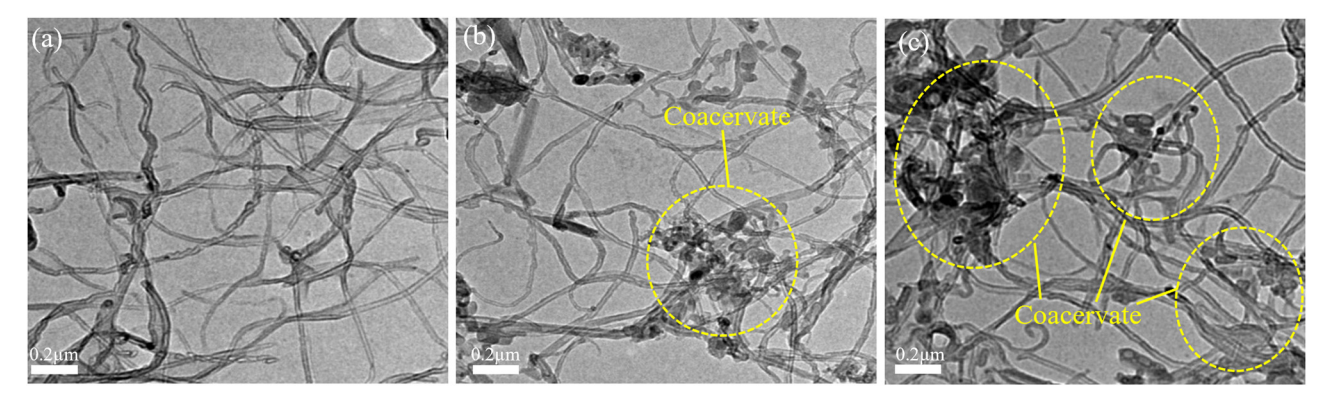


Figure 4: TEM images of CNT suspensions (0.05 g of CNTs) with different dispersants: (a) PVP, (b) GA, and (c) SDBS.

shown in Figure 4(b). SDBS is an anionic surfactant with hydrophobic groups dominated by dodecyl phenyl groups and hydrophilic groups dominated by sulfonic acid groups. However, due to its strong foaming properties during the ultrasonic process, which weakens the homogeneous state of the suspension, the agglomeration of CNTs is extremely severe, as shown in Figure 4(c). In summary, based on the comparison and analysis of micromorphology, the dispersion effect of the CNT suspension prepared with PVP as the surfactant was greater than that of the other two groups.

3.2 Influence of different dispersants on the stability of CNT suspensions under natural standing conditions

According to the mix ratio shown in Table 1 and the preparation process shown in Figure 2, six groups of CNT suspensions were prepared using SDBS, GA, and PVP as dispersants. The results for the above six groups of suspensions after standing for 90 days at room temperature are shown in Figure 5. The six groups of CNT suspensions had no stratification, no sedimentation, uniform blackness, and good dispersion stability. The supernatants of the six groups of samples shown in Figure 5 were diluted at the same ratio and placed in a colorimetric dish, as shown in Figure 6. Figure 6 shows that the blackness of the PVP-CNT suspension and SDBS-CNT suspension is slightly greater than that of the GA-CNT suspension, indicating that PVP and SDBS have better dispersion effects. The supernatants of the six groups of CNT suspensions were extracted, and the absorbance at 260 nm was measured. The variation in the absorbance of the CNT suspensions with different dispersants over time is shown in Figure 7. Figure 7 shows that the absorbance of the different suspensions gradually decreased with increasing time. The dispersion stability of the PVP-CNT suspension was the greatest within 90 days, and the absorbance drop ratios of the PVP-CNT suspensions



Figure 5: CNT suspensions after allowing to stand for 90 days.



Figure 6: CNT suspensions after dilution.

with the two CNTs were 13.75 and 22.41%. The stability of the SDBS-CNT suspension was the worst, and the absorbance drop ratios of the SDBS-CNT suspensions with the two CNTs were 29.17 and 28.72%. The absorbance drop ratios of the GA-CNT suspensions doped with the two CNTs were 24.84 and 17.43%, and the stabilities of the above two suspensions were between those of the other two suspensions.

3.3 Influence of different dispersants on the stability of the CNT suspensions with centrifugal separation

Six groups of aqueous CNT suspensions were reprepared using SDBS, GA, and PVP as dispersants. The 1-PVP and 2-PVP samples had CNT contents of 0.02 and 0.05 g, respectively, and the PVP content was 0.1 g. The rest have the same meaning. Some of the six reprepared groups of samples were poured into centrifuge tubes and centrifuged at

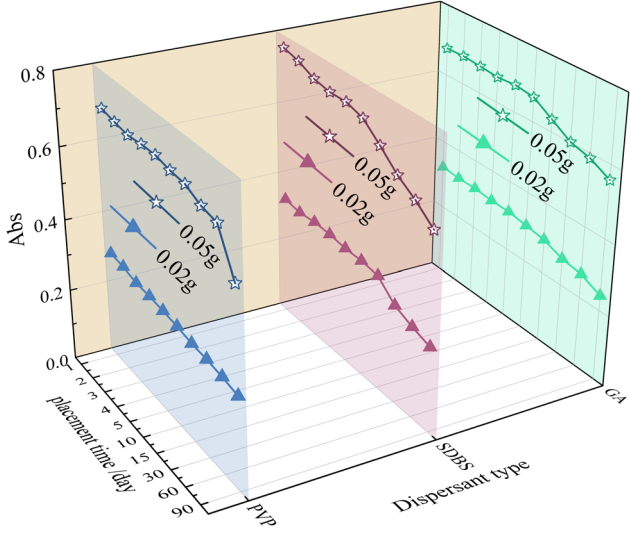


Figure 7: Trend of the absorbances of the CNT suspensions over time.

5,000 rpm using a desktop high-speed centrifuge. After centrifugation for 10 min, the samples were removed for observation. Due to the high concentration of the CNT suspension and agglomeration of CNTs to form cell clusters, no stratification phenomenon or precipitates were observed, and the chemical reaction and diffusion process of the relevant cell clusters can be explored based on the nonlinear Fokker-Planck equation [36]. After centrifugation for 60 min, the supernatant of each sample was diluted to the same concentration, and the absorbance was measured. The absorbance at a wavelength of 260 nm was measured, and the drop ratio was calculated, as shown in Figure 8. Figure 8 shows that the absorbance of the aqueous CNT suspensions prepared with SDBS, GA, and PVP as dispersants decreased significantly before and after centrifugation. After centrifuging the CNT suspensions prepared with PVP as the dispersant, the absorbance of the 1-PVP and 2-PVP suspensions decreased by 27.6 and 36.1%, respectively, the absorbance of the 1-SDBS and 2-SDBS suspensions decreased by 51.9 and 45.9%, respectively, and the absorbance of the 1-GA and 2-GA suspensions decreased by 42.0 and 44.5%, respectively. The absorbance reduction ratio observed in 2-PVP and 2-GA suspensions is greater than that in 1-PVP and 1-GA suspensions. The reason for this lies in the increase in CNT content, which renders the nonionic surfactants PVP and GA unable to fully cover all CNT surfaces, resulting in a larger decrease in absorbance. In contrast, SDBS, an anionic surfactant, utilizes electrostatic repulsion as its primary dispersion mechanism to prevent CNT agglomeration. At high concentrations, SDBS forms micelles or aggregates, which are more prone to settling with CNTs during centrifugation. This leads to a significant reduction in the concentration of CNTs in the

supernatant, subsequently causing a substantial decrease in absorbance. This finding is in agreement with the results reported by Abreu *et al.* [37]. The decrease in the absorbance of the CNT suspension prepared with PVP as the dispersant after centrifugation was the smallest, indicating that the CNT suspension with PVP as the dispersant had better stability.

After centrifuging the CNT suspension six times, it was filtered through filter paper to obtain the CNTs. The CNTs attached to the centrifuge tube were dried and weighed together. The proportion of the filter residue for each sample after centrifugation was obtained by dividing the weight by the original content of CNTs in each sample, as shown in Figure 9. Figure 9 shows that the proportion of filter residue for the 1-GA suspension was the highest, reaching 84.5%, while the proportion of filter residue for the 2-PVP suspension was 58%. The proportion of filter residue for the SDBS suspension is between that of the other two suspensions. From the perspective of the proportion of filter residue for the suspension after centrifugation, the PVP suspension had better stability than did the other two suspensions. The reason for this is that the polymeric chains of PVP can form stable interactions with the surface of CNTs, enabling effective dispersion of CNTs even at high concentrations, thereby reducing agglomeration during centrifugation. Additionally, the shear forces and centrifugal forces generated during centrifugation may contribute to further dispersing some of the originally agglomerated CNTs. These redispersed CNTs may remain suspended in the solution after centrifugation. During the suction filtration process, the SDBS suspension produced a large amount of foam due to its own characteristics and

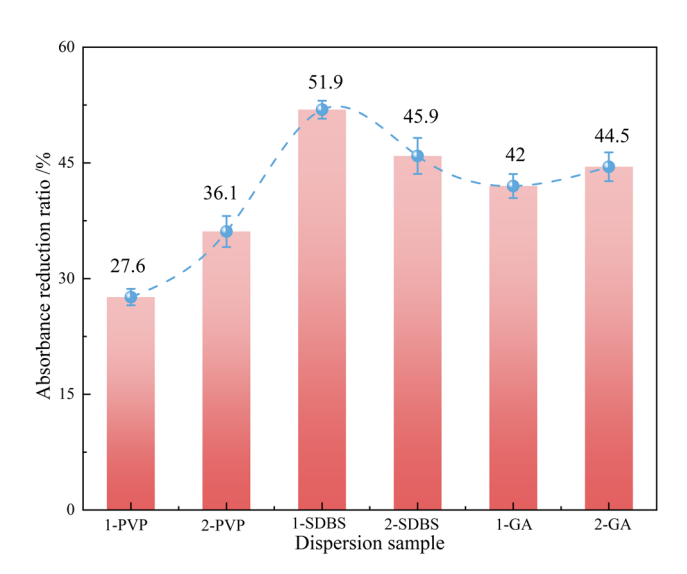


Figure 8: Absorbance drop ratio of the CNT suspensions.

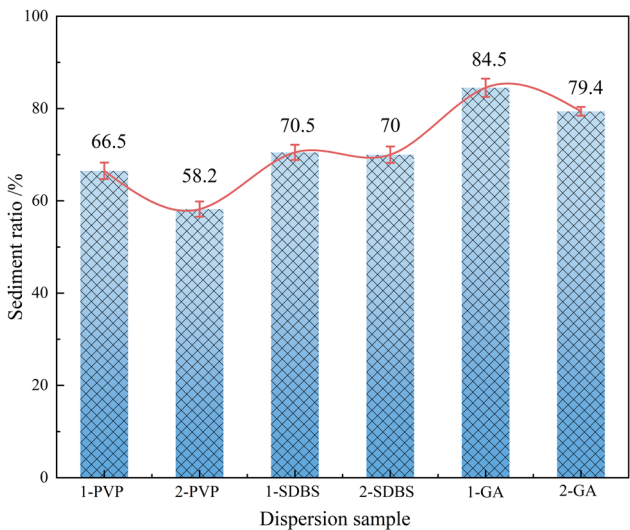


Figure 9: Filter ratio of the CNT suspensions.

8 — Shanxiu Huang et al. DE GRUYTER

airflow movement, as shown in Figure 10(a), which is similar to the phenomenon observed during ultrasonic dispersion, as shown in Figure 10(b). This situation is not conducive to the stability of the SDBS suspension. Therefore, SDBS is not suitable for use as a dispersant for CNTs alone, and it is advisable to use it with a defoamer.

3.4 Optimization of the preparation parameters of the CNT suspension

Based on the above research, PVP was selected as the dispersant, and the CNT content was 0.05 g. According to the factor levels shown in Table 2, nine groups of CNT suspensions were prepared following the process shown in Figure 2(a). After the suspension was incubated for 24 h, the supernatant was collected and diluted to the same concentration to determine the absorbance. The test results are shown in Table 3. The orthogonal test can be performed to analyze the degree and order of influence of various influencing factors on the investigation index. The orthogonal test performed in this analysis is as follows: First, the average value and range of the index of each level of the influencing factors were calculated, and then the primary and secondary order of the influence of each factor on the index according to the size of the range was determined. The influence of each factor level on the index was analyzed according to the relationship between the factor level and the average value of the index. The ranges of the indices of the three influencing factors, A, B, and C, are 0.155, 0.535, and 0.739, respectively. The order of influence of each factor on the absorbance of the CNT suspension was as follows: ultrasonic power (C) had the greatest influence, ultrasonic dispersion time (B) had the second greatest

Table 3: Optimization results of the preparation parameters

| Number | Α | В | С | D (Blank column) | Absorbance |
|--------|----------------|----------------|----------------|------------------|------------|
| 1 | A ₁ | B ₁ | C ₁ | D ₁ | 2.748 |
| 2 | A_1 | B_2 | C_2 | D_2 | 3.782 |
| 3 | A_1 | B_3 | C_3 | D_3 | 3.581 |
| 4 | A_2 | B_1 | C_2 | D_3 | 3.496 |
| 5 | A_2 | B_2 | C_3 | D_1 | 4.109 |
| 6 | A_2 | B_3 | C_1 | D_2 | 2.971 |
| 7 | A_3 | B_1 | C_3 | D_2 | 3.759 |
| 8 | A_3 | B_2 | C_1 | D_3 | 3.514 |
| 9 | A_3 | B_3 | C_2 | D_1 | 3.248 |
| | | | | | |

influence, and the mass ratio of dispersant to CNTs (A) had the smallest influence.

The relationships between the mass ratio of dispersant to CNTs, the ultrasonic dispersion time, the ultrasonic power level, and the absorbance of the CNT suspension are shown in Figure 11. As shown in the figure, with an increasing dispersant doping ratio, the absorbance of the CNT suspension first increased and then decreased. This may be because an excessive PVP content leads to an increase in the osmotic pressure of the micelles after the surface adsorption of the CNTs becomes saturated, which increases the viscosity of the CNT suspension and causes the attraction between CNTs to increase again. When the dispersion equilibrium of CNTs is disrupted, the CNT suspension no longer exists in a stable and uniform distribution state, ultimately leading to a weakening of the dispersion effect of PVP. With increasing ultrasonic dispersion time, the absorbance of the CNT suspension first increases and then decreases. When the ultrasonic dispersion time is 20 min, the absorbance of the suspension reaches the maximum value, indicating that insufficient or excessive ultrasonic dispersion time will affect the dispersion effect of the CNT suspension. As a significant



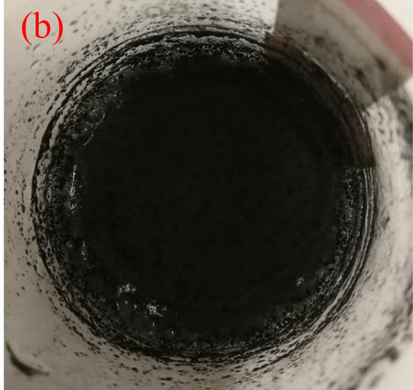
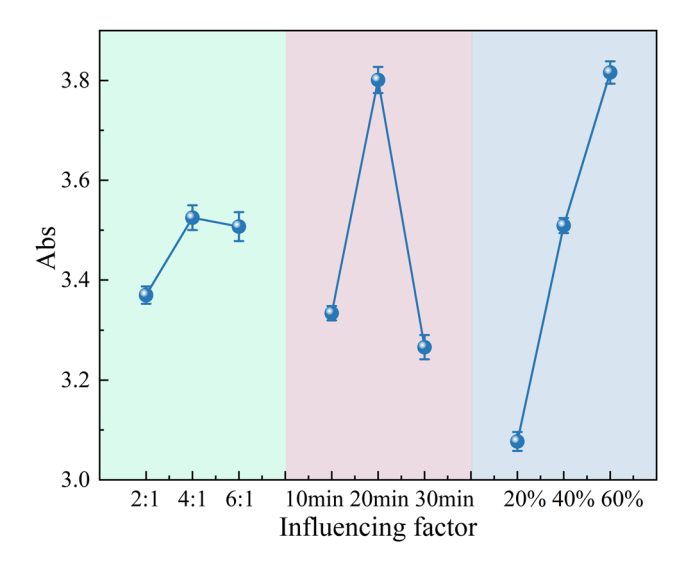


Figure 10: Foaming in the SDBS suspension during the filtration and ultrasonication process: (a) filtration and (b) ultrasonication.



DE GRUYTER

Figure 11: Relationship between the absorbance of the CNT suspensions and different influencing factors.

influencing factor, the absorbance of the CNT suspension increases with increasing ultrasonic power, indicating that higher ultrasonic power can effectively overcome the van der Waals forces between CNTs and improve their dispersion effect.

Absorbance was used as the evaluation index in this orthogonal experiment performed to optimize the preparation parameters of the CNT suspensions. According to the Beer-Lambert law, the absorbance of a CNT suspension is proportional to its concentration, so the concentration of the suspension can be reflected by the absorbance. The greater the absorbance of the CNT suspension and the greater the concentration of the suspension, the greater the dispersion effect of the CNTs. Figure 11 shows that when PVP was used as the dispersant to prepare the CNT suspension used in this article, the optimal preparation parameters were a dispersant:CNT mass ratio of 4:1 and an ultrasonic dispersion time of 20 min. Since the absorbance of the suspension increased with increasing ultrasonic power, additional tests were carried out on the ultrasonic power used to ultrasonicate the suspension at a dispersant: CNT mass ratio of 4:1 and an ultrasonic dispersion time of 20 min. The absorbances of the CNT suspensions at different ultrasonic powers is shown in Figure 12. As shown in Figure 12, with increasing ultrasonic power, the absorbance of the CNT suspension also increases, and the increase is large when the ultrasonic power is between 30 and 40%, which is partly attributed to the enhancement of desorption, this is, as the ultrasonic power increases, more adsorbed substances are desorbed from the surface of the CNTs, which results in the exposure of more active sites on the surface of the CNTs, and thus enhances the

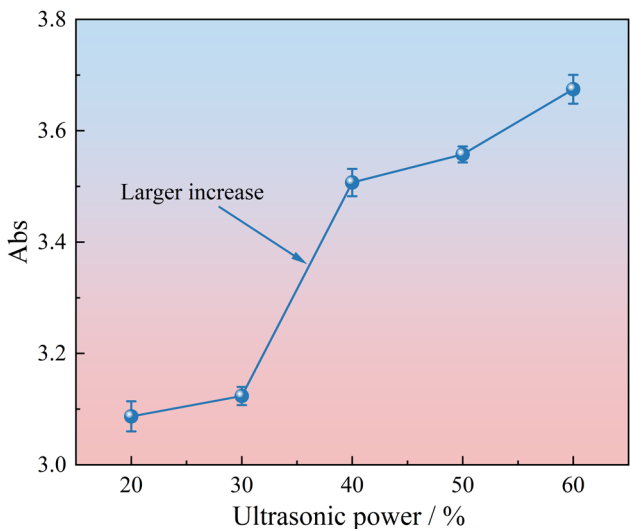


Figure 12: Relationship between the absorbance of the CNT suspensions and ultrasonic power.

CNTs' ability to absorb light. The absorbance is the highest when the ultrasonic power is 60%, and the dispersion effect of CNTs is the greatest. In the additional test, the ultrasonic power was increased to 70%, but too high of an ultrasonic power resulted in cavitation, resulting in a large number of small bubbles in the suspension and many CNTs hanging on the wall, as shown in Figure 13. Suspension preparation could not be completed at this ultrasonic power ratio.

4 Application of the optimization parameters of the CNT suspensions

4.1 CNTC preparation and experiments

First, PVP was added to a beaker containing distilled water and stirred with a glass rod until completely dissolved. Then, CNTs were added to the surfactant solution, and the magnetic stirrer was initially stirred and then moved to the ultrasonic cell grinder for ultrasonic dispersion. The preparation parameters were set according to the preparation parameters shown in Section 3.4. After dispersion, the beaker mouth was closed with a plastic film for use. According to the mix ratio of CNTC shown in Table 4, the weighed raw materials were added to the mixer according to the gravel, sand, and cement, and slow mixing was carried out for 2 min. Then, high-speed mixing was carried out for 3 min. During agitation, the CNT suspensions and water were slowly added. Then, the mixed slurry was put into a



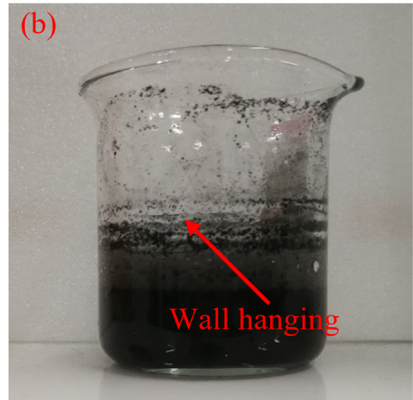


Figure 13: Cavitation and wall hanging phenomena at a high ultrasonic power: (a) cavitation and (b) wall hanging.

cylindrical mold whose inner wall was coated with release oil, and the mold was placed on the shaking table for 30 min before grinding. Finally, after curing in a standard environment for 24 h, concrete samples with CNT contents (mass fraction) of 0, 0.05, 0.10, and 0.30% were prepared by putting the mold into a standard curing room for 27 days. The diameter of the CNTC samples was 50 mm, and the height was 100 mm. The test process is shown in Figure 2(b). An RMT-150B rock mechanics test system was adopted to conduct uniaxial compression tests on the four groups of CNTC samples according to ASTM C39. The axial deformation control loading method was adopted, the axial loading rate was set to 2×10^{-5} m/s, and the corresponding strain rate was 2×10^{-4} s⁻¹. The load sensor with an axial direction of 1,000 kN was used to measure the axial load of the sample with a measurement accuracy of 3 kN, and a displacement sensor with an axial direction of 5 mm was used to measure the axial deformation of the sample with a measurement accuracy of 7.5 µm.

4.2 Stress-strain curve and compressive strength

The stress-strain curves of the CNTC samples under uniaxial compression are shown in Figure 14. The figure

shows that the deformation and failure process of concrete with each CNT content goes through the compaction, elastic deformation, plastic deformation, and failure stages. At the initial stage of loading, the original pores in the concrete samples were gradually compacted, and the stress-strain curves of the concrete samples with different CNT contents clearly exhibited concave shapes [38]. The regularity of the stress-strain curves of the CNTC samples is relatively poor in the compaction stage due to the unavoidable agglomeration of high-content CNTs in the concrete [39], the difference in the flatness of the sample end and the error in the device loading head during the precompaction of the sample. With increasing axial stress, the sample enters the elastic deformation stage, and the stress-strain curve is approximately linear. Figure 14 shows that Young's modulus of the CNTC samples first increases and then decreases with increasing CNT content. When the CNT content is 0, Young's modulus of the CNTC samples is 33.92 GPa. The corresponding Young's modulus are 34.09, 45.45, and 33.15 GPa. Young's modulus of the concrete sample with a CNT content of 0.10% is the largest. Poisson's ratios of the concrete specimens with 0-0.30% CNT content were 0.221, 0.239, 0.240, and 0.233, respectively, which proved the good toughness of the CNTC, and it was also more conducive to the safety and solidity of the structure. With the continuous application of axial load, plastic deformation

Table 4: Mixing ratio of the CNTC samples

| Content (%) | Mass (g) | | | | | |
|-------------|----------|--------|------------|------------------|--------|--------|
| | Water | Cement | River sand | Coarse aggregate | MWCNTs | PVP |
| 0 | 33.95 | 84.78 | 109.51 | 243.74 | 0 | 0 |
| 0.05 | 33.95 | 84.78 | 109.51 | 243.74 | 0.0424 | 0.1696 |
| 0.10 | 33.95 | 84.78 | 109.51 | 243.74 | 0.0848 | 0.3392 |
| 0.30 | 33.95 | 84.78 | 109.51 | 243.74 | 0.2543 | 1.0172 |

DE GRUYTER

begins to occur in the sample. Once the uniaxial compressive strength limit is reached, the sample begins to fail, and the bearing capacity decreases. The incorporation of CNTs has a significant impact on the declining stage of the stress–strain curve. Compared with plain concrete samples, the curves of CNTC samples decrease more slowly, demonstrating obvious ductility. This is in good agreement with the results reported by Zhu *et al.* [40].

The compressive strength of the CNTC under uniaxial compression is shown in Figure 15. As shown in Figure 15, the CNT content has a significant influence on the compressive strength of the CNTC samples. When the CNT content is less than 0.10%, the compressive strength of the sample increases with increasing CNT content [41]. For example, the compressive strength of the concrete sample with a CNT content of 0.10% increased by 9.45 and 7.92 MPa, respectively, compared with that of the concrete with CNT contents of 0 and 0.05%, by 18.15% and 14.78%. When the CNT content exceeds 0.10%, the compressive strength of the CNTC samples decreases with increasing CNT content, and the compressive strength of the CNTC samples decreases by 8.37%. However, the compressive strength of the concrete with CNTs is greater than that of plain concrete. When the CNT content is 0.10%, the compressive strength of the CNTC sample is the highest, this is because the 0.10% CNTs exhibit good dispersibility, enabling them to fully utilize the bridging effect to make the cement paste bond more firmly. However, excessive CNTs can lead to agglomeration, which in turn decreases the strength of the concrete. The same results have also been reported by Ahmad and Zhou [42].

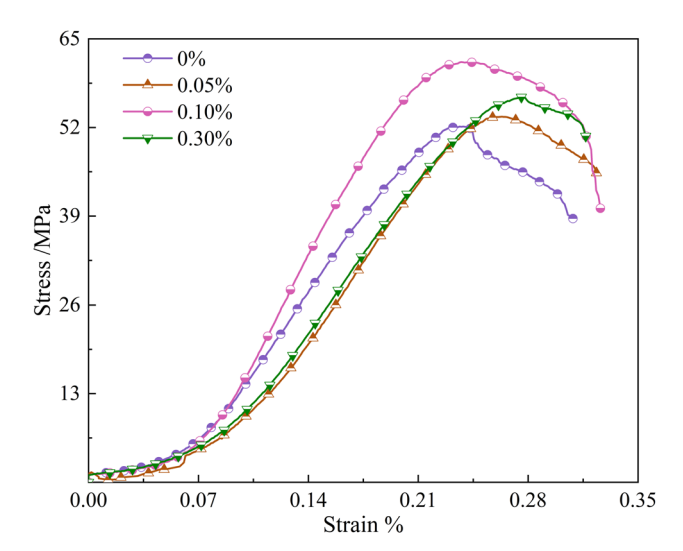


Figure 14: Stress-strain curve of CNTC.

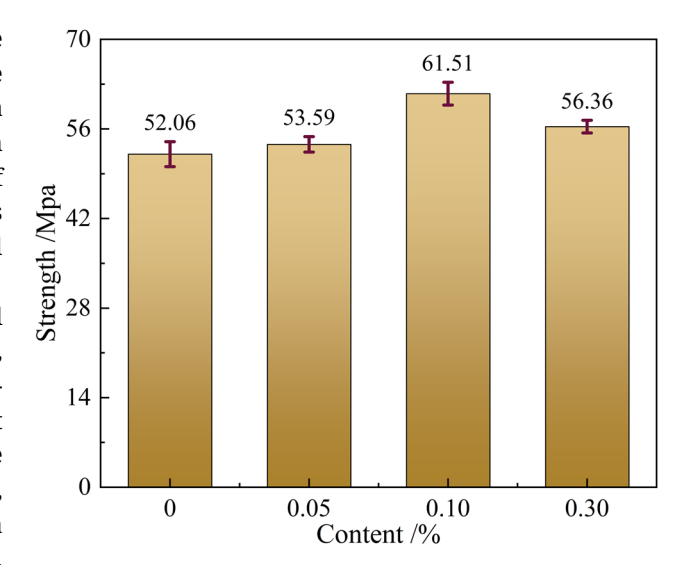


Figure 15: Compressive strength of CNTC.

4.3 Failure mode

The failure modes of concrete with different CNT contents under uniaxial compression are shown in Figure 16. Figure 16 shows that CNT content has a great influence on the failure mode of the concrete samples. Under uniaxial compression, plain concrete exhibits better homogeneity, the bonding friction effect is weak during failure, and the whole frame of the sample is relatively complete during failure. However, with increasing CNT content, the failure of the CNTC is mainly attributed to the overall structural instability, which mainly shows typical shear failure characteristics, and the sample is relatively broken after failure. The concrete sample with 0.10% CNTs shows impact failure characteristics to a certain extent. The reasons for the difference in the failure modes of the concrete samples with different CNT contents are as follows: as a nanoscale reinforcement material, CNTs fill microcracks and pores in the concrete and improve the compaction and strength of the concrete, and this reinforcement effect changes the failure mode of the concrete to a certain extent. For example, 0.10% CNTs can effectively bridge microcracks in concrete and prevent the expansion and connectivity of cracks. Compared with ordinary concrete, CNTC has greater compactness, cohesiveness, and integrity, which will reduce the occurrence of crushing failure and increase the shear failure characteristics when it is damaged. With the continuous increase in axial load, the CNTC reaches its energy storage limit. At this time, the stored elastic strain energy is released sharply during failure, and the energy release rate is high. As a result, the crack friction and slip phenomena of CNTC are significant during failure.

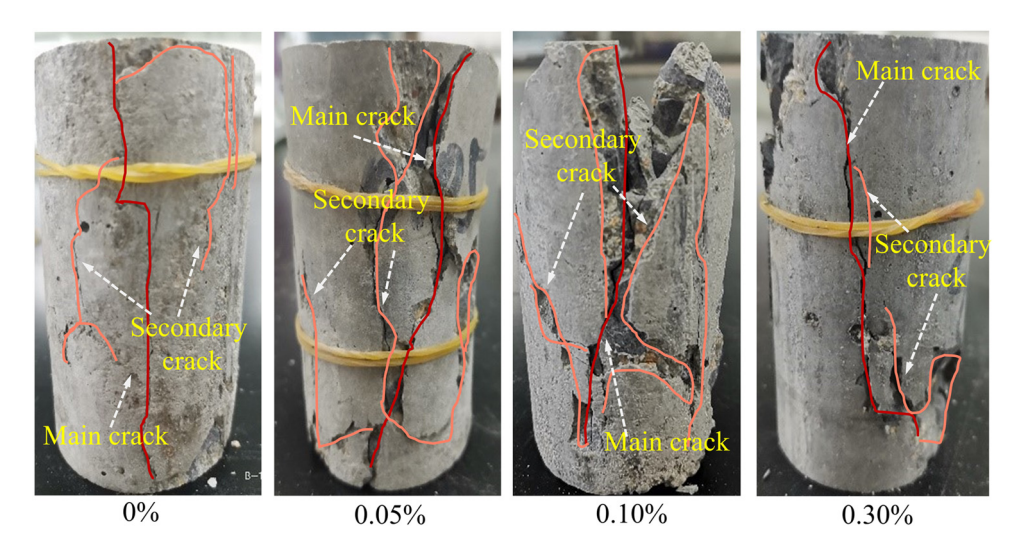


Figure 16: Failure mode of the CNTC.

4.4 Microstructure of the CNTC

The mechanical properties and durability of CNTC are affected by the formation and expansion of microscopic cracks; that is, the macroscopic performance of the material is the inevitable result of changes in its microstructural

characteristics. In this study, SEM and analysis were conducted to observe the microstructure of concrete matrices with different CNT contents. The microstructures of the concrete samples with CNT contents of 0, 0.05, 0.10, and 0.30% are shown in Figure 17(a) and (b). Figure 17(a) shows that there are a large number of micropores and

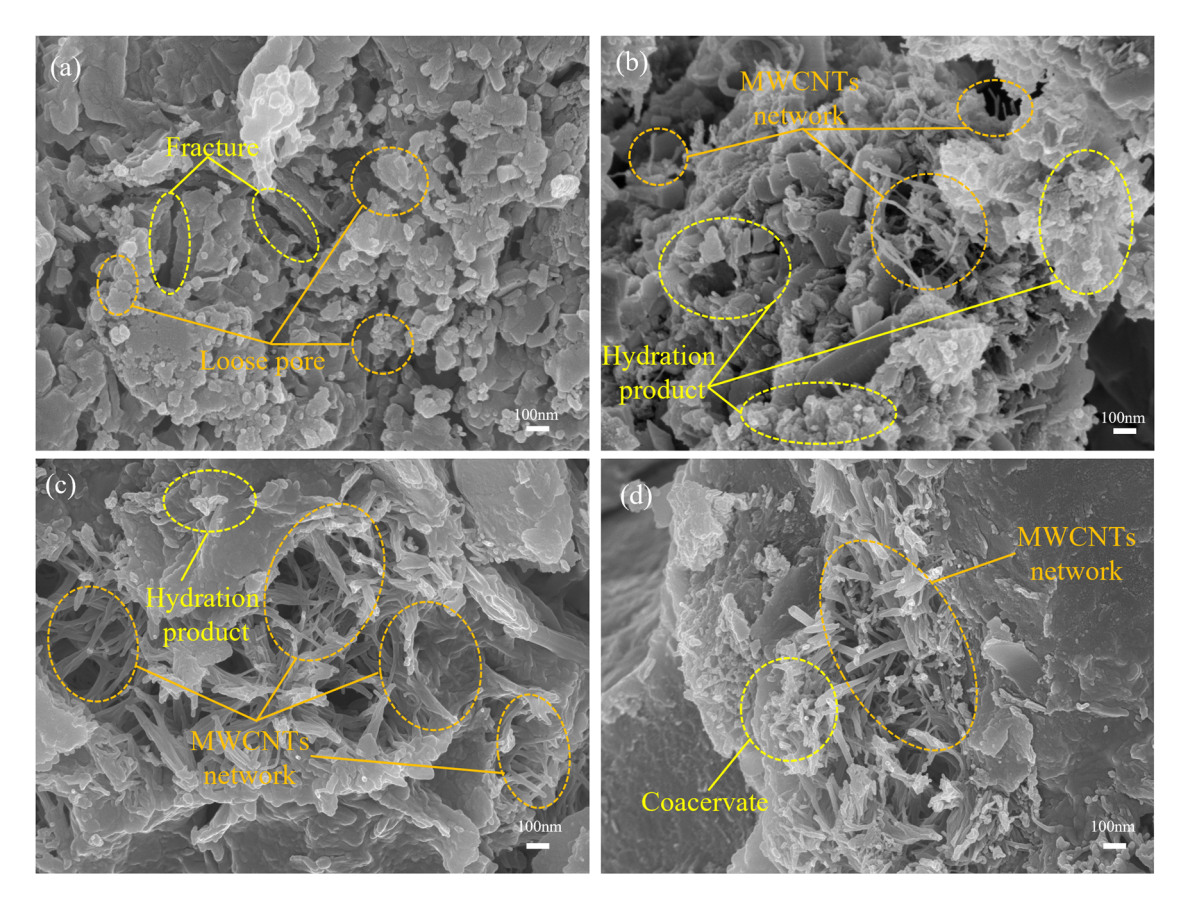


Figure 17: Microstructure of concrete with different CNT contents: (a) 0, (b) 0.05%, (c) 0.10%, and (d) 0.30%.

microcracks in the plain concrete sample. The size of the pores and the opening of the cracks are too large to be completely filled by hydration products, and the matrix is loose and cloud-like, which has a great influence on the macroscopic mechanical properties of concrete. When the CNT content is 0.05%, the dispersion of CNTs in the concrete matrix at room temperature is relatively sparse, as shown in Figure 17(b). The insufficient role of the hydration products and CNTs makes it difficult for the network skeleton of the CNTs to form a long-distance straddle, and CNTs can only play a local strengthening role. In the concrete matrix, most of the irregular voids and cracks still exist, in which case the compressive strength of the concrete is not significantly improved. When the CNT content is increased to 0.1%, the microstructure in Figure 17(c) shows that a larger CNT skeleton is formed, C-S-H hydration products adhere to the CNT clusters and eventually wrap around the CNT clusters, making the CNT interweaving network more uniform and stable, and the matrix microvoids and microcracks transition from loose to dense and effectively filled. The macroscopic mechanical properties are significantly improved [43]. When the CNT content further increases to 0.3%, as shown in Figure 17(d), the CNT network in the CNTC matrix increases the density of the matrix. However, under the influence of van der Waals forces, CNTs intertwine and agglomerate in the concrete matrix, which leads to the inhibition of the growth of cement hydration products in the matrix pores. As a result, the macroscopic mechanical properties of CNTC decrease. Similar results are reported in Wang's literature [44,45].

CNTs can improve the mechanical properties of concrete, and their microscopic mechanism is mainly reflected in the following aspects. CNTs are distributed in the microcracks of the concrete matrix through bridging, as shown in Figure 18(a). On the one hand, when the tip of the microcrack development direction touches the CNTs, crack expansion is inhibited or prevented due to the excellent tensile strength of the CNTs. On the other hand, the interconnected network structure can effectively fill the pores of the matrix, reducing the porosity of the concrete. The number of cracks in the initial concrete hole wall is reduced, thereby reducing the initial defects of the concrete matrix [46,47], as shown in Figure 18(b). From the perspective of energy conversion and consumption, the formation and expansion of cracks is actually a process in which the force exerted by an external load on the material is dispersed and consumed inside the

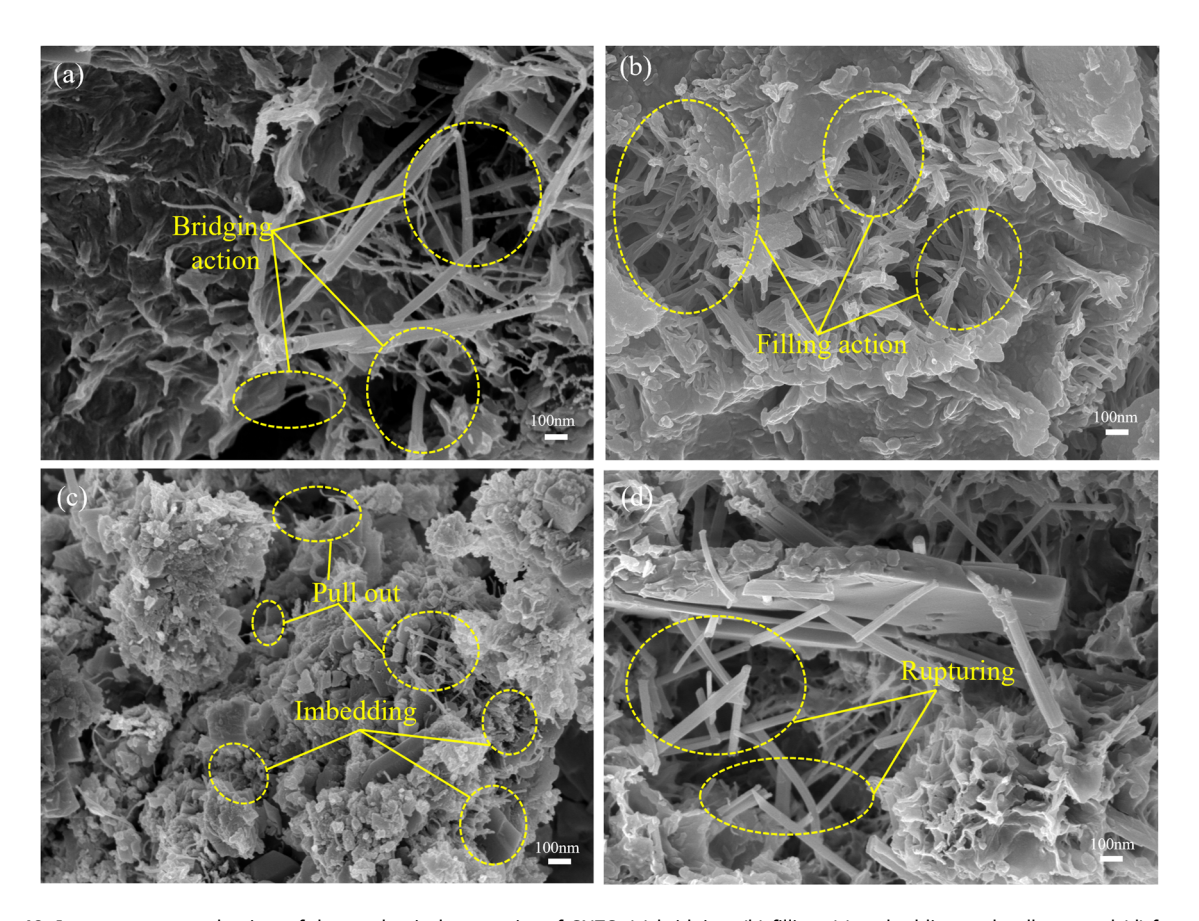


Figure 18: Improvement mechanism of the mechanical properties of CNTC: (a) bridging, (b) filling, (c) embedding and pull out, and (d) fracture.

material. The incorporation of CNTs changes the dispersion and consumption mechanism of the energy generated by the external load inside the concrete matrix, which is partly caused by the appearance and expansion of cracks. The other part is the elongation of the CNTs in the matrix and the loosening or relative slip with the matrix. The work done by weakening or destroying the CNT bridging action within the concrete matrix contributes to the total energy consumption, which increases the energy consumption path, improves the strength of the material and delays the destruction of the material [48–50].

The ports of CNTs in the microcracks are embedded in the hydration products on the surface of the cement particles, and the matrix microcracks are connected so that when the matrix is stretched or compressed, the CNTs can maintain the stability of the cracks to a certain extent through their own mechanical potential energy and the potential energy required to be removed. The bridging effect of CNTs is more effective for crack openings smaller than 1 µm, possibly due to stress and chemical reactions that intensify particle transportation between the nearest neighbor clusters or cells [51]. When the width of the microcrack increases, the bonding strength between the CNTs and the concrete matrix is usually lower than the tensile strength of the CNTs. One end of the CNTs is embedded in the concrete matrix, and the other end is removed. This process needs to overcome the bonding force and friction between the CNTs and the matrix, as shown in Figure 18(c). As shown in Figure 18(d), the main fracture mode is trans-granular fracture, indicating that CNTs have achieved effective dispersion in the concrete matrix and significantly improved the strength of the grains. This fracture mode reflects that CNTs, as bridging points, effectively disperse stress during crack propagation, thereby slowing down the crack propagation speed. This is in good agreement with the research results of Orooji et al. [52]. When the bonding strength between CNTs and the concrete matrix is greater than the tensile strength of CNTs, the CNTs themselves break, but the two ends are still embedded in the concrete matrix; the fracture process is also an important energy-consuming process.

5 Theoretical discussion

With the in-depth research on the application of CNTs in concrete, more kinds of CNTs and their modification methods can be explored in the future to further enhance the mechanical properties, durability, and functionality (such as conductivity, electromagnetic shielding, and so

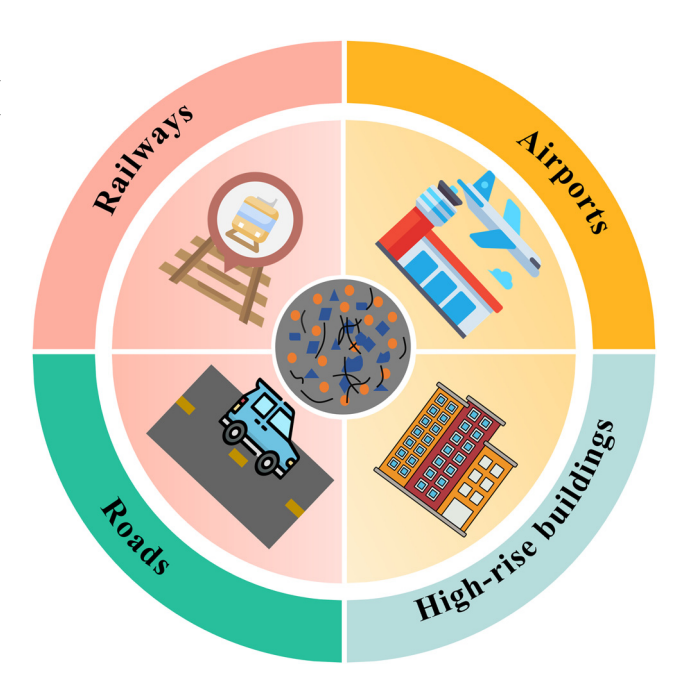


Figure 19: Multi-field application scenarios of CNTC.

on) of concrete, which will provide more innovative space for the next generation of scientists and engineers [53]. The introduction of CNTs has enabled concrete materials to show a wide range of applications in many fields, such as high-rise buildings, railways, roads, and airports (Figure 19). This is important for improving the safety and extending the service life of infrastructure.

This research work is closely linked to the sustainable development goals (SDGs) [54]. Specifically, CNTC indirectly supports the realization of SDG 7 (clean and affordable energy) by improving material properties and reducing energy consumption and carbon emissions. At the same time, its potential to enhance the durability and safety of infrastructures is important for the construction of SDG 11 (Sustainable Cities and Communities). In addition, this study demonstrates adherence to the principles of SDG 12 (Responsible Consumption and Production) and provides new ideas for the sustainable development of the building materials industry. More importantly, this study opens the way for the development of alternative and future advanced materials, inspiring more researchers to devote themselves to research and exploration in this field.

6 Conclusion

This article identified suitable dispersants from PVP, SDBS, and GA, optimized the preparation parameters of the CNT suspensions, and the mechanical properties and microstructure of the

CNTC were studied using an RMT-150B mechanical test system and scanning electron microscopy. The main conclusions are as follows:

- 1) The TEM image of the CNT suspension prepared using PVP as a dispersant showed a uniform CNT cross-linked network, while the TEM image of the suspension prepared using SDBS and GA as dispersants showed CNT agglomeration and CNTs wound into bundles. The nonionic surfactant PVP was more suitable for dispersing CNTs in this study.
- 2) After 90 days of static treatment, the absorbance reduction ratios of PVP-CNT suspensions at two different CNT contents were 13.75 and 22.41%, respectively. For SDBS-CNT suspensions, the absorbance reduction ratios were 29.17 and 28.72%. Meanwhile, the absorbance reduction ratios of GA-CNT suspensions were 24.84 and 17.43%. After centrifugal separation, the absorbance reduction ratios of PVP-CNT suspensions were 27.6 and 36.1%, respectively. The absorbance reduction ratios of SDBS-CNT suspensions were 51.9 and 45.9%. For GA-CNT suspensions, the absorbance reduction ratios were 42.0 and 44.5%. The filtration fraction of the PVP-CNT suspension present after centrifugal separation was significantly smaller than that of the suspensions prepared with the other two dispersants.
- 3) The influence of the ultrasonic power, ultrasonic dispersion time, and dispersing agent-to-CNT mass ratio on the absorbance of the CNT suspension decreased in turn. With increasing mass ratio and ultrasonic dispersion time, the absorbance of the CNT suspension first increased and then decreased, and the absorbance of the CNT suspension increased with increasing ultrasonic power; however, 70% of the ultrasonic power ratio led to cavitation and wall hanging. The optimal parameters for the preparation of CNT suspensions were a mass ratio of PVP to MWCNTs of 4:1, an ultrasonic dispersion time of 20 min, and an ultrasonic power of 60%.
- 4) Under uniaxial compression, the compressive strength of CNTC is greater than that of plain concrete, and the compressive strength of concrete with 0.10% CNT content is the highest, which is 61.51 MPa. The bridge filling effect of CNTs makes the whole structure of the CNTC changes gradually from intact to broken, and the failure mode changes from tensile-shear mixed failure to single-shear failure. The interweaving network of 0.10% CNTs in the concrete matrix is more uniform and stable; when the CNT content increases to 0.30%, the agglomeration of CNTs in some regions of the matrix is obvious. A mass ratio of PVP to MWCNTs of 4:1, an ultrasonic dispersion time of 20 min, and an ultrasonic power of 60% are the

optimum parameters for preparing CNT suspensions, resulting in a significant and high-quality dispersion effect, which lays a foundation for its efficient application in building materials.

Funding information: The authors would like to acknowledge the financial support by the National Key Research and Development Program of China (No. 2023YFC3805903), Doctoral Foundation of Henan Polytechnic University (No. B2024-34), and commissioned scientific research of China Construction Seventh Engineering Bureau Co., Ltd (No. H22-661).

Author contributions: Conceptualization, methodology, validation, investigation, and writing - original draft: Shanxiu Huang; Conceptualization, data analysis, supervision, validation, and writing, revising: Huikuan Li; supervision, and data analysis: Fenghui Gao; experimental design, and data analysis: Weijie Guo; investigation, supervision, and writing - review & editing: Jiaqi Guo. All authors have accepted responsibility for the entire content of this manuscript and approved its submission.

Conflict of interest: The authors state no conflict of interest.

Data availability statement: The datasets generated and/ or analyzed during the current study are available from the corresponding author on reasonable request.

References

- [1] Dang VP, Kim DJ. Effects of nanoparticles on the tensile behavior of ultra-high-performance fiber-reinforced concrete at high strain rates. J Build Eng. 2023;63:105513.
- Guo H, Wang H, Xue H, Li H, Li Y, Wei L. Study on damage dete-[2] rioration mechanism and service life prediction of hybrid fibre concrete under different salt freezing conditions. Constr Build Mater. 2024;435:136688.
- Chung DDL. Cement reinforced with short carbon fibers: a multi-[3] functional material. Compos Part B-Eng. 2000;31(6):511-26.
- Li H, Wang Y, Liu S, Zhang L, Sun S, Xie K. Investigation on piezo-[4] resistivity of self-sensing cementitious composites containing nano carbon fillers under water content variations. Constr Build Mater. 2024;438:137169.
- Zhou ZJ, Yang ZF. Study on the smart property of carbon coated nylon fiber-reinforced concrete composites. J Chin Ceram Soc. 2001;2:192-5 (in Chinese).
- Li C, Qian J, Tang Z. Study on properties of mechanically sensitive concrete with steel slag. China Concr Cem Prod. 2005;2:5-8 (in Chinese).
- Kim JK, Kim JS, Ha G, Kim Y. Tensile and fiber dispersion performance of ECC (engineered cementitious composites) produced

- with ground granulated blast furnace slag. Cem Concr Res. 2007;37(7):1096–105.
- [8] Sivakumar G, Mohanraj K, Barathan S. Dielectric study on fly ash blended cement. E-J Chem. 2008;6(1):231–6.
- [9] Xiong G, Deng M, Huang H, Tang M. Absorbing and mechanical properties of cement-based composites with nano-titanic oxide absorbent. Adv Mater Res. 2010;177:558–61.
- [10] Wang J, Ye H, Sun Z, Chen W. Experiment on the crack and deflection of basalt fiber reinforced concrete beams. Adv Mater Res. 2011;243–249:1058–61.
- [11] Nimbagal V, Banapurmath NR, Sajjan AM, Patil AY, Ganachari SV. Studies on hybrid bio-nanocomposites for structural applications. J Mater Eng Perform. 2021;30:6461–80.
- [12] Patil M, Hunasikai SG, Mathad SN, Patil AY, Hegde CG, Sudeept MA, et al. Enhanced O2/N2 separation by QuaternizedMatrimid/Multiwalled carbon nanotube mixed-matrix membrane. Heliyon. 2023;9(11):e21992.
- [13] Iijima S. Carbon nanotubes: past, present, and future. Phys B: Condens Matter. 2002;323(1–4):1–5.
- [14] Jongvivatsakul P, Thongchom C, Mathuros A, Prasertsri T, Adamu M, Orasutthikul S, et al. Enhancing bonding behavior between carbon fiber-reinforced polymer plates and concrete using carbon nanotube reinforced epoxy composites. Case Stud Constr Mat. 2022;17:e01407.
- [15] Roopa AK, Hunashyal AM, Patil AY, Kamadollishettar A, Patil B, Soudagar ME, et al. Study on interfacial interaction of cementbased nanocomposite by molecular dynamic analysis and an RVE approach. Adv Civ Eng. 2023;2023(1):8404335.
- [16] Musale A, Hunashyal AM, Patil AY, Kumar R, Ahamad T, Kalam MA, et al. Study on nanomaterials coated natural coir fibers as crack arrestor in cement composite. Adv Civ Eng. 2023;2024(1):6686655.
- [17] Singh A, Kumar S, Nivedan A, Kumar S. Temperature-dependent ultrafast response and π -plasmon dynamics in single-walled carbon nanotubes. J Phys Chem Lett. 2021;12(1):627–32.
- [18] Fu Q, Zhou ZM, Wang ZH, Huang J, Niu DT. Insight into dynamic compressive response of carbon nanotube/carbon fiber-reinforced concrete. Cem Concr Comp. 2022;129:104471.
- [19] Jing Y, Lee JC, Moon WC, Ng JL, Yew MK, Chu MY. Mechanical properties, permeability and microstructural characterisation of rice husk ash sustainable concrete with the addition of carbon nanotubes. Heliyon. 2024;10(12):e32780.
- [20] Nuaklong P, Boonchoo N, Jongvivatsakul P, Charinpanitkul T, Sukontasukkul P. Hybrid effect of carbon nanotubes and polypropylene fibers on mechanical properties and fire resistance of cement mortar. Constr Build Mater. 2021;275:122189.
- [21] Xing G, Xu Y, Huang J, Lu Y, Miao P, Chindasiriphan P, et al. Research on the mechanical properties of steel fibers reinforced carbon nanotubes concrete. Constr Build Mater. 2023;392:131880.
- [22] Cwirzen A, Habermehl-Cwirzen K, Nasibulin AG, Kaupinen EI, Mudimela PR, Penttala V. SEM/AFM studies of cementitious binder modified by MWCNT and nano-sized Fe needles. Mater Charact. 2009;60(7):735–40.
- [23] Xin X, Pang JY, Li WZ, Wang YT, Yuan J, Xu G. Dispersing carbon nanotubes in aqueous solutions of trisiloxane-based surfactants modified by ethoxy and propoxy groups. J Surfactants Deterg. 2015;18:163–70.
- [24] Li Y, He C, Song D, Fan M, Guo L, Zhai X, et al. Highly dispersed and stable Schiff base nickel catalyst on multi-walled carbon nanotubes promote ethylene oligomerization. Chem Eng J. 2024;497:154447.

- [25] Yazdanbakhsh A, Grasley Z, Tyson B, Abu Al-Rub RK. Distribution of carbon nanofibers and nanotubes in cementitious composites. Transp Res Rec. 2010;2142(1):89–95.
- [26] Makar J, Margeson J, Luh J. Carbon nanotube/cement composites early results and potential applications. Proceedings of the 3rd International Conference on Construction Materials: Performance. Innov Struct Implic; 2005.
- [27] An SK, Kim KY, Lee JU. Reinforcement of cement nanocomposites through optimization of mixing ratio between carbon nanotube and polymer dispersing agent. Polymers-Basel. 2024;16(3):16030428.
- [28] Bu LX, Li JJ, Gao LL, Yin LH. Dispersion of multi-walled carbon nanotubes in solution with surfactant SDBS. Plat Finish. 2019;41(7):10–3 (in Chinese).
- [29] Chinese National Standard GB/T 14685-2011. Pebble and crushed stone for construction. Beijing: China Building Materials Federation; 2011 (in Chinese).
- [30] Chinese National Standard GB 175-2007. Common Portland cement. Beijing: Ministry of Industry and Information Technology; 2007 (in Chinese).
- [31] Chinese National Standard GB 5749-2006. Standards for Drinking Water Quality. Beijing: National Health Commission; 2006 (in Chinese).
- [32] Sobolkin A, Mechtcherine V, Khavrus V, Maier D, Mende M, Ritschel M, et al. Dispersion of carbon nanotubes and its influence on the mechanical properties of the cement matrix. Cem Concr Comp. 2012;34(10):1104–13.
- [33] Hu T, Jing H, Li L. Humic acid assisted stabilization of dispersed single-walled carbon nanotubes in cementitious composites. Nanotechnol Rev. 2019;8(1):513–22.
- [34] Kim Y, Hong JS, Moon SY, Hong JY, Lee JU. Evaluation of carbon nanotubes dispersion in aqueous solution with various dispersing agents. Carbon Lett. 2021;31(6):1327–37.
- [35] Liu J, Suh H, Jee H, Xu J, Nezhad EZ, Choi CS, et al. Synergistic effect of carbon nanotube/TiO₂ nanotube multi-scale reinforcement on the mechanical properties and hydration process of portland cement paste. Constr Build Mater. 2021;293:123447.
- [36] Bahari A, Sadeghi-Nik A, Roodbari M, Sadeghi-Nik A, Mirshafiei E. Experimental and theoretical studies of ordinary Portland cement composites contains nano LSCO perovskite with Fokker-Planck and chemical reaction equations. Constr Build Mater. 2018;163:247–55.
- [37] Abreu B, Pires AS, Guimarães A, Fernandes RM, Oliveira IS, Marques EF. Polymer/surfactant mixtures as dispersants and noncovalent functionalization agents of multiwalled carbon nanotubes: Synergism, morphological characterization and molecular picture. J Mol Liq. 2022;347:118338.
- [38] Chen T, Wang ZH, Wang A, Bai E, Zhu X. Comparative study on the static and dynamic mechanical properties and micro-mechanism of carbon fiber and carbon nanofiber reinforced concrete. Case Stud Constr Mat. 2023;18:e01827.
- [39] Bahari A, Sadeghi-Nik A, Shaikh F, Sadeghi-Nik A, Cerro-Prada E, Mirshafiei E, et al. Experimental studies on rheological, mechanical, and microstructure properties of self-compacting concrete containing perovskite nanomaterial. Struct Concr. 2022;23(1):564–78.
- [40] Zhu P, Jia QH, Li ZX, Wu Y, Ma ZJ. Theoretical model for the stress–strain curve of CNT-reinforced concrete under uniaxial compression. Buildings-Basel. 2024;14(2):14020418.
- [41] Mohsen MO, Alansari M, Taha R, Senouci A, Abutaqa A. Impact of CNTs' treatment, length and weight fraction on ordinary concrete mechanical properties. Constr Build Mater. 2020;264:120698.

- [42] Ahmad J, Zhou ZG. Properties of concrete with addition carbon nanotubes: A review. Constr Build Mater. 2023;393:132066.
- [43] Yao Y, Lu H. Mechanical properties and failure mechanism of carbon nanotube concrete at high temperatures. Constr Build Mater. 2021;297:123782.
- [44] Wang Q, Gao Y, Zhao J, Hu Z, Liu W, Lv H, et al. Acoustic emission based experimental study on mechanical properties and damage analysis of carbon nanotube reinforced fiber shotcrete. J Build Eng. 2024;93:109850.
- [45] Gao FF, Tian W, Wang Z, Wang F. Effect of diameter of multi-walled carbon nanotubes on mechanical properties and microstructure of the cement-based materials. Constr Build Mater.
- [46] Liew KM, Kai MF, Zhang LW. Carbon nanotube reinforced cementitious composites: an overview. Compos Part A-Appl S. 2016;91(1):301-23.
- [47] Xu SL, Liu JT, Li QH. Mechanical properties and microstructure of multi-walled carbon nanotube-reinforced cement paste. Constr Build Mater. 2015;76:16-23.
- [48] Chen SJ, Zou B, Collins F, Zhao XL, Majumber M, Duan WH. Predicting the influence of ultrasonication energy on the reinforcing efficiency of carbon nanotubes. Carbon. 2014;77:1-10.

- [49] Chowdhury SC, Hague BZ, Okabe T. Modeling the effect of statistical variations in length and diameter of randomly oriented CNTs on the properties of CNT reinforced nanocomposites. Compos Part B-Eng. 2012;43(4):1756-62.
- Parveen S, Rana S, Fangueiro R, Paiva MC. Microstructure and mechanical properties of carbon nanotube reinforced cementitious composites developed using a novel dispersion technique. Cem Concr Res. 2015:73:215-27.
- Bahari A, Sadeghi-Nik A, Cerro-Prada E, Sadeghi-Nik A, Roodbari M, Zhuge Y. One-step random-walk process of nanoparticles in cement-based materials. J Cent South Univ. 2021;28(6):1679-91.
- Orooji Y, Derakhshandeh RM, Ghasali E, Alizadeh M, Asl MS, Ebadzadeh T. Effects of ZrB2 reinforcement on microstructure and mechanical properties of a spark plasma sintered mullite-CNT composite. Ceram Int. 2019;45(13):16015-21.
- [53] Kai C, Chang J, Feo L, Chow CL, Lau D. Developments and applications of carbon nanotube reinforced cement-based composites as functional building materials. Front Mater. 2022;9:861646.
- [54] Sun H, Amin MN, Qadir MT, Arifeen SU, Iftikhar B, Althoey F. Investigating the effectiveness of carbon nanotubes for the compressive strength of concrete using AI-aided tools. Case Stud Constr Mat. 2024;20:e03083.